Research Article | Vol. 26, No. 9 | 30 Apr 2018 | OPTICS EXPRESS 11125
Optics EXPRESS

Validation of the particle size distribution obtained with the laser in-situ scattering and transmission (LISST) meter in flow-through mode

EMMANUEL BOSS,[1,*] NILS HAËNTJENS,[1] TOBY K. WESTBERRY,[2] LEE KARP-BOSS,[1] AND WAYNE H. SLADE[3]

[1] *University of Maine, School of Marine Sciences, 5706 Aubert Hall, Orono, ME 04473, USA*
[2] *Oregon State University, Department of Botany and Plant Pathology, 2055 Cordley Hall, Corvallis, OR, 97331, USA*
[3] *Sequoia Scientific, Inc, 2700 Richards Rd., Suite 107, Bellevue, WA 98005, USA*
[*] *emmanuel.boss@maine.edu*

Abstract: High spatial and temporal resolution estimates of the particle size distribution (PSD) in the surface ocean can enable improved understanding of biogeochemistry and ecosystem dynamics. Oceanic PSD measurements remain rare due to the time-consuming, manual sampling methods of common particle sizing instruments. Here, we evaluate the utility of measuring particle size data at high spatial resolution with a commercially-available submersible laser diffraction particle sizer (LISST-100X, Sequoia Scientific), operating in an automated mode with continuously flowing seawater. The LISST PSD agreed reasonably well with discrete PSD measurements obtained with a Coulter Counter and data from the flow-through sampling Imaging Flow-Cytobot, validating our methodology. Total particulate area and Volume derived from the LISST PSD agreed well with beam-attenuation and particulate organic carbon respectively, further validating the LISST PSD. Furthermore, When compared to the measured spectral characteristics of particulate beam attenuation, we find a significant correlation. However, no significant relationship between the PSD and spectral particulate backscattering was found.

OCIS codes: (010.4450) Oceanic optics; (290.5850) Scattering, particles; (280.3420) Laser sensors; (290.3200) Inverse scattering.

References and links

1. T. S. Kostadinov, D. A. Siegel, and S. Maritorena, "Retrieval of the particle size distribution from satellite ocean color observations," J. Geophys. Res. **114**, C09015 (2009).
2. R. J. W. Brewin, N. J. Hardman-Mountford, S. J. Lavender, E. E. Raitsos, E. Hirata, J. Uitz, E. Devred, A. Bricaud, A. Ciotti, and B. Gentili, "An intercomparison of bio-optical techniques for detecting phytoplankton size class from satellite remote sensing," Rem. Sens. Enviro., **115**, 325–339, (2011).
3. Y. C. Agrawal and H. C. Pottsmith, "Instruments for particle size and settling velocity observations in sediment transport," Mar. Geol. **168**, 89–114 (2000).
4. R. A. Reynolds, D. Stramski, V. M. Wright, and S. B. Wozniak, "Measurements and characterization of particle size distributions in coastal waters," J. Geophys. Res. **115** C08024 (2010).
5. B. Barone, M. J. Church, D. M. Karl, R. M. Letelier, and A. E. White, "Particle distributions and dynamics from laser diffraction in the North Pacific Subtropical Gyre," J. Geophys. Res. **120**, 3229–3247 (2015).
6. F. Volz, "Die Optik und Meterologie der atmospharischen Trubung," Ber. Dtsch. Wetterdienstes **2**, 3–47 (1954).
7. A. Morel, "Diffusion de la lumière par les eaux de mer. Résultat expèrimentaux et approch théorique," in *Optics of the Sea*, AGARD Lecture Series 61, NATO, Paris, pp. 3.1.1–76 (1973).
8. E. Boss, M. S. Twardowski, and S. Herring, "Shape of the particulate beam attenuation spectrum and its relation to the size distribution of oceanic particles," Appl. Opt. **40**, 4885–4893 (2001).
9. E. Boss, W. S. Pegau, W. D. Gardner, J. R. V. Zaneveld, A. H. Barnard., M. S. Twardowski, G. C. Chang, and T. D. Dickey, "Spectral particulate attenuation and particle size distribution in the bottom boundary layer of a continental shelf," J. Geophys. Res. **106**, 9509-9516 (2001).
10. W. H., Slade, and E. Boss, "Spectral attenuation and backscattering as indicators of average particle size," Appl. Opt. **54**(24), 7264–7277 (2015).

#320735 https://doi.org/10.1364/OE.26.011125
Journal © 2018 Received 26 Jan 2018; revised 9 Apr 2018; accepted 9 Apr 2018; published 16 Apr 2018

Optics EXPRESS

11. G. Dall'Olmo, T. K. Westberry, M. J. Behrenfeld, E. Boss, and W. H. Slade, "Significant contribution of large particles to optical backscattering in the open ocean," Biogeosciences **6**, 947–967 (2009).
12. W. H., Slade, E. Boss, G. Dall'Olmo, M.R. Langner, J. Loftin, M.J. Behrenfeld, C. Roesler, and T.K. Westberry, "Underway and moored methods for improving accuracy in measurement of spectral particulate absorption and attenuation", J. Atmos. Ocean. Tech., **27**(10), 1733–1746 (2010).
13. E. Boss, M. Picheral, T. Leeuw, A. Chase, E. Karsenti, G. Gorsky, L. Taylor, W. Slade, J. Ras, and H. Claustre, "The characteristics of particulate absorption, scattering and attenuation coefficients in the surface ocean; Contribution of the Tara Oceans expedition," Methods Ocean. **7**, 52–62 (2013).
14. Sequoia Scientific, Inc., "Processing LISST-100 and LISST-100X data in MATLAB," https://www.sequoiasci.com/article/processing-lisst-100-and-lisst-100x-data-in-matlab/.
15. P. Traykovski, R. J. Latter, and J. D. Irish, "A laboratory evaluation of the laser in situ scattering and transmissometery instrument using natural sediments," Mar. Geol. **159**, 355–367 (1999).
16. L. Karp-Boss, L. Azevedo, and E. Boss, "LISST-100 measurements of phytoplankton size distribution: evaluation of the effects of cell shape," Limnol. Oceanogr. Meth. **5**, 396–406 (2007).
17. E. Boss, W. H. Slade, M. Behrenfeld, and G. Dall'Olmo, "Acceptance angle effects on the beam attenuation in the ocean," Opt. Express **17**(3), 1535–1550 (2009).
18. H. C. van de Hulst, *Light Scattering by Small Particles* (John Wiley and Sons, 1957; reprint, Dover, 1981).
19. M. J. Behrenfeld and E. Boss, "Beam attenuation and chlorophyll concentration as alternative optical indices of phytoplankton biomass," J. Mar. Res. **64**, 431–451 (2006).
20. R. J. Olsen and H. Sosik, "A submersible imaging-in-flow instrument to analyze nano-and microplankton: Imaging FlowCytobot," Limnol. Oceanogr. Methods **5**, 195–203 (2007).
21. E. A. Moberg and H. Sosik, "Distance maps to estimate cell volume from twoâĂŘdimensional plankton images," Limnol. Oceanogr. Methods **10**, 278–288 (2012).
22. J. R. Graff, T. K. Westberry, A. J. Milligan, M. B. Brown, G. Dall'Olmo, V. van Dongen-Vogels, K. M. Reifel and M. J. Behrenfeld, "Analytical phytoplankton carbon measurements spanning diverse ecosystems," Deep Sea Res. I, **102**, 16–25 (2015).
23. S.B. Moran, M. A. Charette, S. M. Pike, and C. A. Wicklund, "Differences in seawater particulate organic carbon concentration in samples collected using small- and large-volume methods: the importance of DOC adsorption to the filter blank," Mar. Chem. **67**, 33–42 (1999).
24. K. Davidson, E. C. Roberts and L.C. Gilpin, "The relationship between carbon and biovolume in marine microbial mesocosms under different nutrient regimes," Eur. J. Phycol., **37**, 501–507 (2002).
25. T.K. Westberry, G. Dall'Olmo, E. Boss, M.J. Behrenfeld, and T. Moutin, "Coherence of particulate beam attenuation and backscattering coefficients in diverse open ocean environments," Opt. Express **18**, 15419–15425 (2010).
26. G. Dall'Olmo, E. Boss, M.J. Behrenfeld, and T.K. Westberry, "Particulate optical scattering coefficients along an Atlantic Meridional Transect," Opt. Express **20** 21532–21551 (2012).
27. I. Cetinic, N. Poulton, and W. H. Slade. "Characterizing the phytoplankton soup: pump and plumbing effects on the particle assemblage in underway optical seawater systems," Opt. Express, **24**, 20703–20715 (2016)
28. D. A. Siegel, K. O. Buesseler, M. J.Behrenfeld, C. R. Benitez-Nelson, E. Boss, M. Brzezinski, A. Burd, C. A.Carlson, E. A. D'Asaro, S. C. Doney, MJ Perry, R. H. R. Stanley and D. K. Steinberg, "Prediction of the Export and Fate of Global Ocean Net Primary Production: The EXPORTS Science Plan," Front. Mar. Sci. **3**, 22 (2016).

1. Introduction

The particle size distribution (PSD) in aquatic environments conveys important characteristics for both biogeochemistry and ecosystem dynamics (e.g., particle surface processes, rising and settling speeds, prey-predator interactions). Therefore, there is substantial interest in obtaining particle size information over broad scales in the surface ocean.

A number of algorithms to retrieve particle size information from satellite ocean color remote sensing data have been proposed, albeit with only limited validation due to the poor coverage of in-situ measurements [1, 2]. Traditional bench-top particle sizers, such as the Coulter Counter (Beckman Coulter, Brea, CA, USA) are not equipped for continuous automated sampling and measurements of discrete water samples are time consuming. *In-situ* observational technologies, such as the Laser In Situ Scattering and Transmission (LISST) instrument (LISST- 100X, Sequoia Scientific, Bellevue, WA, USA) allow rapid automated counting and sizing of particles. LISST instruments have been successfully used for over 20 years to obtain high resolution vertical profiles of PSD, yet spatial coverage in surface waters to match with satellite ocean color remote sensing data remains sparse.

Although the LISST was initially designed for sediment transport studies in particle dense

Optics EXPRESS

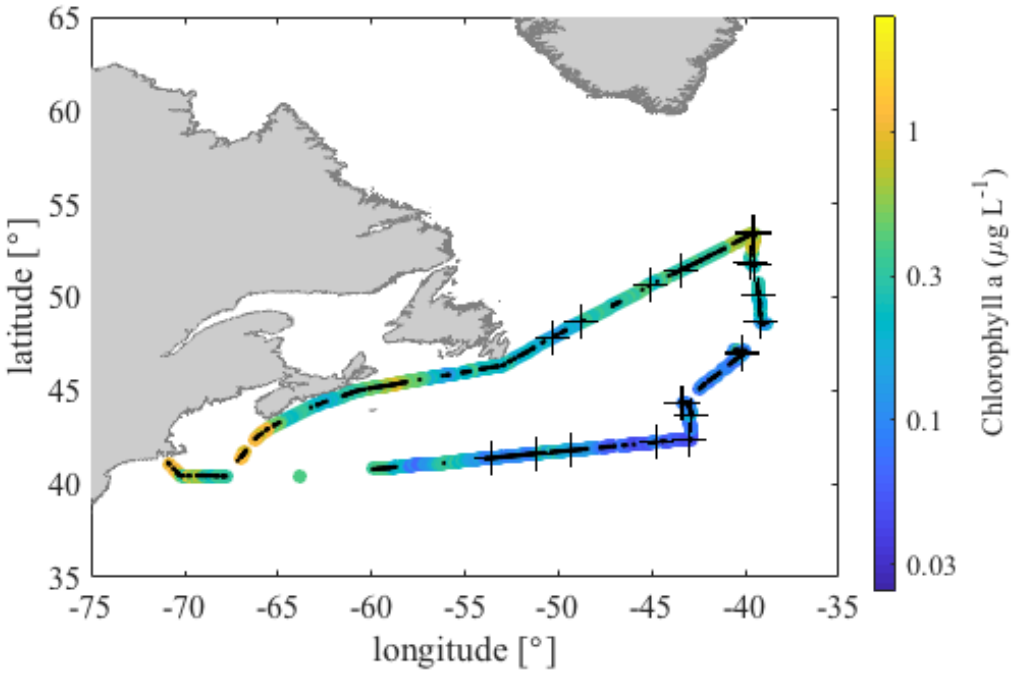

Fig. 1. Cruise track during NAAMES03 where data is available. Large color dots display chlorophyll a concentration (see colorbar), small black dots are where LISST data are available and a + symbol denote where the locations of 24 Coulter Counter-LISST match-ups.

bottom boundary layers [3], the incorporation of dynamic gains has extended its utility to clearer ocean waters [4,5]. Here, we test the potential of operating the LISST in a shipboard flow-through system, where water is pumped continuously aboard a research vessel and passed through a series of instruments to obtain size information over large areas of the ocean. Measurements were conducted during a cruise in the North Atlantic Ocean and particle size spectra obtained by the LISST are evaluated and validated using optical theory and independent size measurements collected with a Coulter Counter (CC) and an imaging flow-CytoBot (IFCB). We also compare the power-law fit exponents of the resulting LISST PSD spectra with those obtained from spectral particulate beam-attenuation and particulate-backscattering measurements. These latter properties have been shown to contain information related to the steepness of the PSD both theoretically [6–8] and in *in-situ* observations in coastal environments and in bottom boundary layers [9, 10], but has not been linked to size spectra in the surface ocean.

2. Methods

2.1. Flow-through system

In September 2017 we deployed a flow-through system for measuring surface ocean optical properties aboard the R/V Atlantis during an expedition to the North Atlantic (Fig. 1). The system was similar to previously described experiments [11–13]. One unique aspect of these systems is the switching between sampling of whole unfiltered seawater to 0.2-μm filtered water for ten minutes of every hour. The filtered water measurements, if stable between two consecutive periods, provide a calibration (by subtraction) for particulate optical measurements [12]. Stability of this baseline calibration is also monitored with an in-line CDOM fluorometer.

Optics EXPRESS

The LISST was adapted to the flowing seawater system using a manufacturer-provided 100-mL black flow-through chamber, minimizing contamination by ambient light. To maximize signal to noise of measurements in very clear waters, the LISST was configured to record continuously at a fixed rate, with each output sample consisting of an average of 250 raw detector measurements (using the "Measurements per Average" setting in LISST-SOP software), resulting in an output sample period of approximately 10 s. LISST measurements were further averaged to 10 min bins and quality controlled by removal of outliers (e.g., bubbles). For each bin, averages were calculated using only data between the 15^{th} to 75^{th} percentiles, resulting in approximately 36 output samples averaged within each 10 min bin. The reason for this asymmetric averaging window was to eliminate outlying data (particularly positive spikes due to bubbles).

For a typical flow rate of 5 L/min, the residence time in the 100 mL sample chamber is 1.2 s, and it is reasonable to assume that each 10 s output sample represent about 8 independent measurements of the entire sample chamber volume. Thus, since each 10 min bin represents an average of 36 output samples, a conservative estimate of the volume observed in each bin is 20 L.

The last 3 min of the filtered periods were used as clear water background measurements (referred to as *zscat*) for both the LISST's scattering and attenuation measurements. Data from other optical instruments (ac-s and Eco-BB3) were similarly quality-controlled and binned to 1 min bins [13].

2.2. LISST measurements and inferred particle size distribution

LISST data processing was conducted using standard procedures [3, 14], including corrections for attenuation along the laser path, variation of the source output (laser reference), detector area correction (referred to as *dcal*) and subtraction of the background (*zscat*). Particle beam attenuation $c_p(670)$ was calculated from transmission measured by a pinhole detector in the beam (0.0269° acceptance angle) and laser reference detector. For most applications, Sequoia provides a standard detector area correction (32 values for correction of the detector array) that is applied to the raw detector array scattering measurements [3, 14]. However, for this study, the LISST was calibrated post-cruise using NIST-traceable sub-micron beads at the manufacturer, where it was determined that the *dcal* for the two outer detector rings should be adjusted. This step significantly improved the agreement between CC and LISST at the smaller-size edge of the derived PSDs. Using this factor the calibrated amount of light on each detector is obtained (*cscat*). For both attenuation and scattering measurements the background measurements were based on linearly interpolating the measurements of filtered seawater performed ten minute of every hour.

We used the manufacturer-provided spherical particle (Mie-scattering) inversion to obtain the volume distribution (VD, $\mu L\, L^{-1}$ or ppm), from which we computed the differential volume size distribution (VSD, $\mu L\, L^{-1}\, \mu m^{-1}$) by dividing the value in each size bin by the bin width. Differential area size distribution (ASD, $m^{-1}\, \mu m^{-1}$) are also calculated from the VSD, assuming particles are spheres. Instrument output is in 32 size bins ranging from 1.25 µm to 250 µm. It has been observed that inversion results can be problematic for the first and last few bins due to the effect of scattering by particles outside this size range [10, 15] and we therefore focus on particles >2.03 µm (the 3rd smallest LISST size bin). The data also has large uncertainties at the higher end of the size range due to the presence of large rare particles. The LISST optical measurement is most sensitive to a particle's cross-sectional area and hence, for non-spherical particles, will represent a wider size distribution than that from an instrument whose measurement depends on particle volume [16].

The magnitude of the PSD depends on a calibration parameter obtained by the manufacturer, termed the "Volume Conversion Coefficient" (VCC). This conversion factor is needed to scale the output of the PSD inversion, because the kernel matrix is in relative units, not in terms of particle volume or mass. The VCC is determined at the factory by measuring a known concentration of standard test dust (nominal 5-10 µm fraction Arizona Test Dust, Particle Technology Inc.,

Optics EXPRESS

Arden Hills, MN) with the LISST instrument and determining a scaling factor such that the summed output of the numerical version, divided by the VCC, is equal to the known volume concentration (assuming a solid particle density of 2.65 g cm^{-3}). There is uncertainty in the VCC due to difficulty in mixing the test dust, as well as measurement error in the test dust mass and liquid volume, and is estimated to be on the order of 10% based on replication with a single sensor.

We cross-validated the beam-attenuation measurements of the LISST with those obtained through concurrent ac-s measurements (see below). We expect the two estimates to be very well correlated with the LISST attenuation being larger due to a significantly smaller acceptance angle [17] (LISST acceptance angle is 0.0269° compared to 0.93° for ac-s). To test the consistency of the PSD obtained (and hence the VCC) we compared predictions from optical theory with the LISST measurements. For a population of particles in suspension dominated by particles that are much larger than the wavelength of measurement, optical theory predicts that the average attenuation efficiency factor $\overline{Q_c} = c_p/\overline{G}$ (i.e., the ratio of particle beam attenuation to the total particle geometric area, $\overline{G}$) should be approximately between 2 to 3 (Fig. 32, p.177, in [18]). This prediction is consistent with previous observations in oceanic environments, using a variety of methods. For example, [4] found $\overline{Q_c}$ in coastal waters to range from 2.08 to 2.64 using LISST measurements (λ = 532 nm) of both PSD and beam attenuation (Note that within the LISST instrument, beam attenuation is measured by a separate photodetector, independent of the the near-forward scattering measurements used for the PSD inversion). Similarly [19] found $\overline{Q_c}$ to be roughly 1.5 to 2 using PSD measured by a CC and attenuation obtained from a transmissometer in the Equatorial Pacific. Thus, we can evaluate the consistency of the LISST inversion estimates from this dataset by calculating the average attenuation efficiency factor [unitless] for each measurement:

$$\overline{Q_c} = \frac{c_p(670)}{\sum_i ASD(D_i)\Delta D_i}, \tag{1}$$

where the sum is over all 32 size bins, and ΔD_i is the width of the i-th size bin.

As part of the post cruise calibration at the manufacturer, 38 − 45 and 75 − 90 μm general purpose Whitehouse Scientific seaved glass beads were measured with the sensor with a resulting Q_c of 1.92 and 1.84 respectively, which is less than 10% of the theoretically expected value of 2.03 ± 0.03 and within the uncertainty of the VCC. This is an additional validation the LISST VCC used in this study.

2.3. Spectral optical measurements

In addition to the LISST-100X (Type B, λ = 670 nm, 5-cm pathlength), we also employed a hyperspectral spectrophotometer and transmissometer (ac-s, Sea-Bird Scientific, Bellevue, WA, USA, formerly WET Labs, 25-cm pathlength), a three-channel backscattering meter (Eco-BB3, λ = 470, 532, 650 nm, Sea-Bird/WET Labs), and a CDOM fluorometer (WETStar, Sea-Bird/WET Labs). A CTD (Sea-Bird, SBE45) continuously recorded temperature and salinity of the flow-through seawater. The ac-s and backscattering data were processed similar to [11–13] to obtain the particulate beam attenuation spectra, $c_p(\lambda)$ (units m^{-1}), and backscattering spectra, $b_{bp}(\lambda)$ (units m^{-1}). One difference in processing from previous studies is that here we used the relative change in CDOM fluorescence (measured continuously) to interpolate between periods of filtered measurements (rather than a simple linear interpolation). Along-track chlorophyll-a concentration was estimated from the 676 nm absorption line-height as in [13].

Optical theory for a power-law PSD (e.g., PSD $\sim D^{-\xi}$) of non-absorbing, spherical particles with diameter D spanning the size range from zero to infinity, predicts power-law spectra for the inherent optical properties (IOPs) $c_p(\lambda)$ and $b_{bp}(\lambda)$ (e.g., $c_p(\lambda) \sim \lambda^{-\gamma_{cp}}$ and $b_{bp}(\lambda) \sim \lambda^{-\gamma_{bbp}}$). Further, the spectral slope is related algebraically to the PSD slope, specifically, $\gamma_{cp} = \xi - 3 = \xi_v$

Optics EXPRESS

[6, 7] (ξ_v is the power-law fit exponent of the VSD, see below). The size-spectra relationship without the assumption of non-absorbing particles over an infinite size range has been examined [8], and size-dependence of the spectral slope has also been observed in field data [9, 10]. For this dataset, non-linear least squares fits were used to obtain power-law exponents (γ_{cp} and γ_{bbp}) of these spectra as function of wavelength for comparison with LISST measurements.

2.4. Coulter counter measurements

To compare PSD measurements from the LISST with CC measurements, thirty four discrete samples were collected from the same flow-through system and 2 mL water samples were typically measured in triplicate (we report their averages) using a CC Multi-Sizer 3 with a 70 µm aperture. The output of the CC is the number of particles in each of 50 logarithmically-spaced bins ranging from 1.4 µm to 42 µm. However, for many spectra, there were no particles measured beyond 17.35 µm. We therefore interpolate the CC and LISST-based VSDs to the common size range $17.35 > D > 2.03$ µm (CC bins 6-37) for the comparison described below. The CC measures changes in impedance as particles pass through the aperture and provide a measure of particle volume, for which an equivalent spherical diameter can be estimated. Uncertainties in measurement based on replication varied, on average, from less than 20% in the smaller sizes to 50% in the larger size bins compared with the LISST.

Valid match-ups between LISST and CC measurements required that they were collected within ±1 h of each other, a compromise between sample numbers and variability associated with temporal mismatch. This criterion excluded 10 CC measurements, leaving 24 discrete match-ups. All LISST samples within the ±1 h window surrounding a CC measurement were averaged for match-up.

2.5. IFCB measurements

We also installed an Imaging Flow-CytoBot (IFCB) in the in-line system to image chlorophyll containing particles [20]. Every 22min a 5mL sample is drawn into the instrument and particles that contain chlorophyll (detected through fluorescences) are imaged and their properties stored (e.g. estimated volume [21]). We use the volume distribution of the imaged particles to build an IFCB-based PSD for each approximately 5mL sample, which we compare to that of the LISST. While the IFCB captures only a subset of the particles 'seen' by the LISST, the significant correlation between the measurements by the two instruments over the large dynamic range that we observed provides additional confidence in the LISST measurements. We compared IFCB measurements from the flow-though system with those collected with the ship's rosette and found no bias in numbers or average particles size suggesting the flow-through system did not affect the phytoplankton population significantly (and by inference, other particles). We expect phytoplankton carbon to be on the order of 10-30% of particulate organic carbon [22], and hence we would expect the volume comparison to be of a similar order of magnitude. Match-up criteria between the IFCB and LISST required that measurements were collected within ± 30 min of each other.

2.6. Particle size parameters

For both the LISST and CC size distributions, median particle size is computed similar to [4],

$$\frac{\int_{D_{min}}^{D_V^{50}} VSD(D)dD}{\int_{D_{min}}^{D_{max}} VSD(D)dD} = 0.5 \tag{2}$$

where $VSD(D)$ is the volume size distribution at diameter D, $D_{min} = 2.03$ and $D_{max} = 17.35$ µm. The integral is computed numerically on data interpolated linearly into 1000 equally spaced diameter between D_{min} and D_{max}.

Optics EXPRESS

The power law exponent of the VSDs (ξ_v) were computed by minimizing the cost function

$$\chi^2 = \sum_i \frac{(VSD(D) - v_0 D_i^{-\xi_v})^2}{\sigma_i^2}, \tag{3}$$

where i is the bin index, v_0 is the VSD amplitude, ξ_v is the exponent of the VSD power-law-fit, and σ_i are the uncertainties for each VSD bin, described in Section 2.7. Note that in our previous works [9, 10] we have computed the PSD power-law-fit exponent, ξ, from both CC and LISST measurements which, for a power-law distributed population of non-absorbing particles is related to VSD exponent by: $\xi = \xi_v + 3$.

2.7. Uncertainties

The relative uncertainties of the CC based on replication have a median of 15% for the full range, and 7% for the restricted range we compare with the LISST. Given that for the LISST we use an inversion product as opposed to a direct measurement of size, it is not simple to a-priori derive size-specific uncertainty for the PSD (used to compute the spectral exponent, σ_i in Eq. (3)). We therefore used three approaches to estimate the uncertainties of the VSD in Eq. (3):

1. Assume a constant uncertainty in the VSD as a function of size (similar to what one assumes when computing a non-linear fit)
2. Assume a constant relative uncertainty in the VSD as a function of size (similar to what one assumes when performing a line fit to a log-linear plot)
3. Obtain an uncertainty by propagating the variability in near-forward scattering within the match-up period through the LISST inversion.

In the rare case where only one LISST VSD was available within the match-up period, we use the average of all standard deviations for the weighting function in Eq. (3). An additional scaling uncertainty (size independent) is that associated with the VCC discussed above.

2.8. Particulate organic carbon

To additionally validate our PSD results we compare them to discrete measurements of particulate organic carbon (POC) taken at the same time as CC samples. POC were collected and calculated using the multiple volume filtrate approach (generally, 0.5 L, 1 L, and 2 L) described in [23].

3. Results and discussion

3.1. Beam-attenuation closure and its relationship to cross-sectional area

Table 1. **Statistics of comparisons of LISST and ac-s derived parameters**

Variables compared	N	ρ (p-value)	$\Sigma(A_i - B_i)/N$	$\Sigma\lvert A_i - B_i\rvert/N$
$c_{p,LISST}$ and $c_{p,ac-s}$	1165	0.67 (p<0.001)	0.04 m^{-1}	0.06 m^{-1}
ξ_v and γ_{cp}	1173	0.55 (p<0.001)	0.12	0.2
D_{avg} and γ_{cp}	1173	-0.31 (p<0.001)		

Particulate beam attenuation estimated from the LISST and ac-s are well correlated, with LISST values being slightly larger (on average by 0.04 m^{-1}, Fig. 2(a), Table 1). This difference is expected given their difference in acceptance angle. The good numerical agreement implies that oceanic particles are less enriched in large particles compared to the coastal environments [17].

Optics EXPRESS

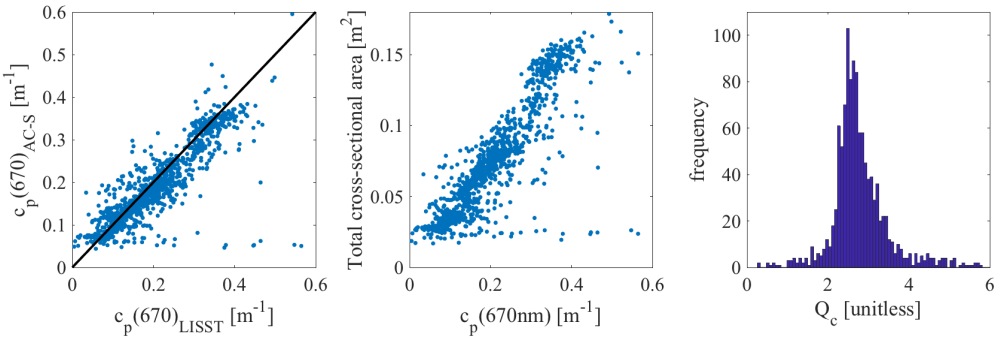

Fig. 2. (a) comparison of 1165 measurements of $c_p(670)$ taken within ±5 min of each other by ac-s and LISST, (b) total-cross-sectional area of particles vs. $c_p(670)$ and (c) histogram of attenuation efficiency factor $Q_c(670)$ based on 1207 10 min-averaged LISST measurements. To focus on the bulk of the data only the lower 96% of the data are displayed.

The LISST beam attenuation is also well correlated with the cross-sectional area inverted from the angular scattering measurements (Fig. 2(b)) and their ratio, the attenuation efficiency factor (Q_c) is within the acceptable theoretical range (Fig. 2, median $Q_c = 2.7$, mean $Q_c = 3.1 \pm 0.05$) indicating that the attenuation and scattering measurements of the LISST are consistent. It also highlights the fact that the majority of particles relevant to attenuation are captured by the LISST scattering measurements (if we missed much of the particulate population the Q_c would have been significantly higher, as the cross-sectional area would have been under-estimated). Ignoring the first and last three bins of the inversion changes the results by approximately 15% (median $Q_c = 3$, mean $Q_c = 3.5 \pm 0.07$).

3.2. *LISST comparison with Coulter counter*

The LISST and CC volume-size-distributions generally agree in shape except for some notable coherent features observed with the LISST which are only found in some CC spectra, namely peaks around 3 µm and 5 µm (Fig. 3). The CC spectra are noisier, which is consistent with being averaged over a smaller sample volume (~6 mL) compared to the LISST (~20 L). In addition, the nature of the LISST inversion tends to produce smooth PSD since the kernel functions that are used to fit the measured scattering data are mostly smooth functions [3].

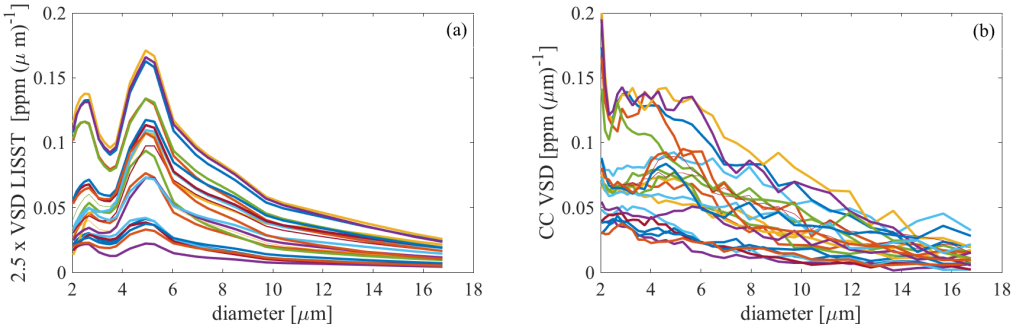

Fig. 3. VSD spectra ($N = 24$) estimated from (a) LISST, and (b) Coulter Counter (CC). All spectra were truncated at 17.35 µm and LISST spectra were linearly interpolated to the exact size-bins of the CC. Note the amplitude of the LISST spectra has been multiplied by 2.5.

Optics EXPRESS

The LISST and CC disagree by about a factor of 2.5 on estimates of total-particulate-volume (ppm) and hence VSD magnitude, but do agree on parameters independent of amplitude such as the median diameter and VSD exponent (Fig. 4(a)). Uncertainties exist in both methods, but this bias in magnitude is significantly larger than previously reported (e.g. [4]). As described in the methods section, the LISST scaling was validated with glass beads after the cruise, which provides us confidence in its amplitude.

In order to further investigate the difference in PSD amplitude, we use Particulate Organic Carbon (POC) measurements together with total particulate volume estimates from the LISST and CC. POC per unit volume is well-constrained for biological particles. A compilation of such values for particles spanning from bacteria, through phytoplankton and to heterotrophic flagellates [24] suggest values should vary from 0.1-0.4 Pg μm^{-3}. Since we expect our recovered total particlate volumes to be an underestimate of the total volume contained within POC (as we only use a limited size range, $17.35 > D > 2.03$), we expect values of this ratio to be higher for our samples (Fig.4(b), and as we saw in [19]). This finding provides another indication that the LISST returns a more realistic estimate of particle concentration that the CC.

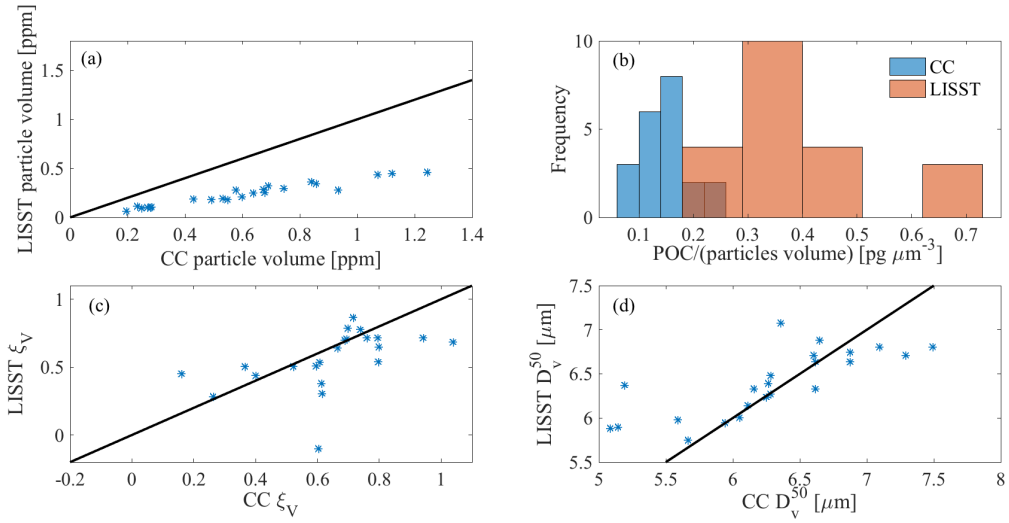

Fig. 4. Comparison of (a) total particulate volume, (b) POC normalized by total particulate volume, (c) power-law exponent and (d) median diameter (based on volume) of Coulter Counter (CC) and LISST measurements taken within one hour of each other. Black lines are the 1:1 lines.

The power-law fits between $17.35 > D > 2.03$ µm converged for 23 of the 24 LISST and CC match-ups. The LISST VSD exponent is on average 0.1 higher than that of the CC with an averaged absolute difference of 0.15 (Fig. 4(c)). Note that these were obtained by assuming that the uncertainty in the LISST VSD is proportional to the magnitude of the VSD for the power-law fit (uncertainty 2 in Section 2.7). The two other uncertainty estimates resulted in a significantly worst match-up with the CC (mean absolute difference of 0.3, 0.15, and 1.41 for uncertainties 1, 2, and 3 respectively).

The median particle diameter is constrained between 5 and 8 µm and agrees well between LISST and CC, with the LISST overestimating by 0.1 µm on average and with an averaged absolute difference of 0.3 µm (Fig. 4(d)), consistent in sign with the bias expected for non-spherical particles.

Optics EXPRESS

3.3. Comparison of LISST with Imaging FlowCytobot

To further investigate the observed amplitude bias between LISST and CC PSD, we also compared LISST and IFCB measurement. Note that the IFCB only counted and sized chlorophyll containing particles. The instruments are well correlated (2) despite the likelihood of some underestimation by the IFCB in the smallest size bin (H. Sosik, personal communication, 2017). The mean ratio of total volume (an indicator of mass) estimated from the IFCB and from the LISST in the 2.9-20.8 µm is 0.18 ± 0.06 which is consistent with 20% of POC being due to chlorophyll containing particles [22] and assuming similar particulate carbon concentration for non-algal-particles and phytoplankton. If instead, the LISST amplitude were equal to that of the CC, only 7.2% of the particles in that size range would contain chlorophyll, which is less likely given surface ocean observations.

Table 2. **Correlation coefficient (r) for 679 comparisons of LISST and IFCB particle areas at different size bins. p<0.0001 for all.**

Size bin [μm]	2.9-20.8	2.9-4.7	4.7-7.7	7.7-12.7	12.7-20.8
r	0.77	0.66	0.71	0.65	0.55

3.4. Comparison of LISST and ac-s

The LISST and ac-s agree well on the value of beam-attenuation at 670nm (Fig. 2(a), Table 1). In addition, the LISST VSD exponents correlate well with the power-law fit exponent of $c_{p,ac-s}(\lambda)$ (Fig. 5(a), Table 1), but the relationship is noisy and γ_{cp} tends to be larger than ξ_v on average (if the particles were non-absorbing spheres, power-law distributed from 0 to inf we would have expected them to be similar [6]). Importantly, this is the first time that γ_{cp} has been found to correlate significantly with a PSD exponent in the open ocean.

The correlation between LISST volume based median particle diameter and the power-law fit exponent of $c_{p,ac-s}(\lambda)$ is weaker (Fig. 5(b), Table 1), yet still significant (but note the smaller dynamic range in D_{avg}). The negative correlation is expected, as $c_p(\lambda)$ spectra tend to flatten as function of wavelength when measured suspension are enriched with larger particles [6–8].

We have conducted a similar comparison with the b_{bp} spectrum but found no significant correlation with the LISST power-law exponent or c_p spectra power-law exponent. This could be due to several reasons, including the stronger effect of absorption on scattering compared to attenuation, and larger uncertainties in backscattering measurements compared to those of attenuation. It is possible that with a better choice of wavelengths (we use 470, 532 and 650 nm) a significant relationship will emerge.

A major caveat in our measurements is that they are all based on analysis of water that has been pumped through the flow-through system and hence, has been subjected to significant turbulent shear stress that is likely to break fragile aggregates and long chains. Comparison of IFCB measurements on water collected from the CTD rosette with that of the flow-through system shows no bias in total concentration or mean size, but one may argue that the process of obtaining water from a rosette is also detrimental to large delicate aggregates. More studies are therefore necessary to establish the presence and magnitude of the bias between undisturbed PSDs in the ocean and those measured through a flow-through system. Comparisons of optical properties in the water and from similar flow-through systems have found no significant differences [25, 26], except when intake pump was an impeller pump [27], suggesting bias in PSD in the open ocean due to the pump are likely small.

Optics EXPRESS

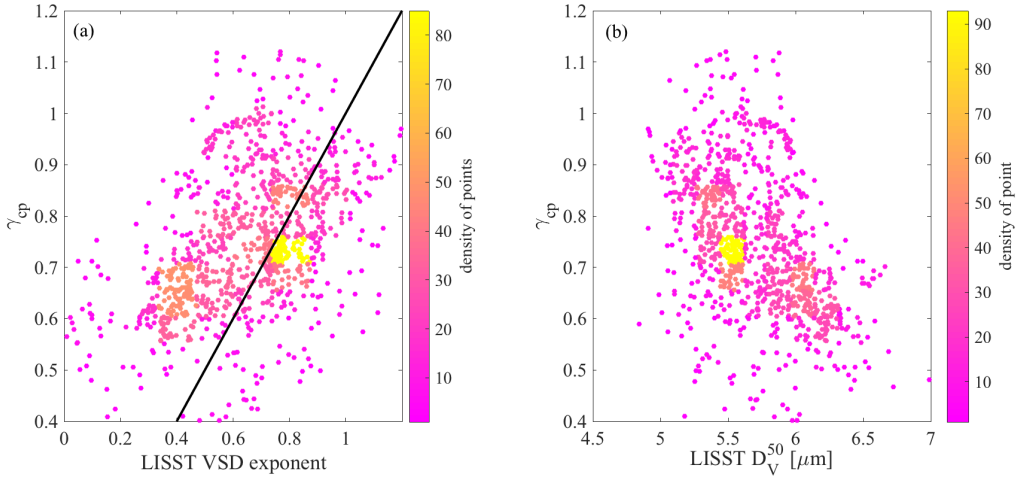

Fig. 5. (a) $c_p(\lambda)$ spectral exponent vs. VSD power-law-fit exponent (b) $c_p(\lambda)$ spectral exponent vs. VSD based median diameter. The color represents the density of points within ranges of value of the variables. In order to better visualize the relationships we have focused in on the data such that in (a) 96% and in (b) 97% of the data are shown.

4. Conclusion

We find that the LISST provides a size distribution that is generally consistent in shape with the CC for the size range considered here, similar to [4]. However, we found that the CC overestimates the LISST size distributions by a factor of 2.5. Post-cruise calibration of the LISST validated the amplitude scaling factor we used. Additionally, When comparing LISST particle volume with that obtained for chlorophyll containing particles with the IFCB for the range 2.9-20.8 µm and with the discrete POC samples, we find LISST PSD estimates to be consistent with reported contributions of phytoplankton to POC and with reported POC to volume ratios of micro-organisms.

In terms of Ocean Color remote sensing inversions, the LISST VSD exponent has been shown to correlate significantly with the exponent of the power-law-fit of the particulate beam-attenuation spectrum, but not that of particulate backscattering. The link to IOP spectra has been one avenue explored to obtain information on size from space (e.g., [1]) and based on our data, seems a promising avenue of inquiry but requiring more work. The lack of correlation with particulate backscattering spectra may be due to a number of reasons including: varying the choice of backscattering wavelengths, lack of data on small particles, or limitations of the assumed power-law size spectra for particles (see [4]).

We have demonstrated the ability to obtain LISST PSD as part of a continuously recording flow-through system in clear oceanic waters spanning a period of weeks. The ongoing reference to 0.2-µm-filtered sea water as a blank provides quantitative estimates of beam attenuation (Fig. 4) as well as size spectra (Fig. 3) that are validated here with other instruments. The method we have developed opens the possibility to obtain size information throughout the world ocean, much as is currently done with optical properties such as spectral beam attenuation and absorption (e.g., [13]). This information is critical for global biogeochemical models and, in particular, for studies regarding particle export from the surface ocean [28]. We caution the readers that in high particulate load waters (e.g. coastal environments and bloom conditions), the PSD of particles passing through a flow-through system could be significantly different from that in the water due to disaggregation.

Optics EXPRESS

Funding

National Atmospheric and Space Administration (NASA) (NNX15AE67G).

Acknowledgments

This data set was collected as part of the NASA NAAMES project. We thank M. Behrenfeld and C. Hostetler for leading NAAMES, J. Graff and P. Graub for support before and during the cruise, and the crew of the R/V Atlantis for all their help with the setup and maintenance of the flow-through system. We thank three anonymous reviewers whose comments have led to an improved manuscript.

Disclosures

WHS: Sequoia Scientific, Inc. (I,E). EB, NH, TKW, LKB declare no conflicts of interest related to this article.